

Determining the impact of WDR5 on the ability of N-MYC to bind chromatin

By

Leigh Bumpous

A Thesis Submitted in Partial Fulfillment of the Requirements for the Degree
of Master of Science

Middle Tennessee State University

December 2022

Thesis Committee:

April Weissmiller, PhD., Chair

Jason Jessen, PhD.

J. Brian Robertson, PhD.

ACKNOWLEDGEMENTS

I want to thank my loving God and my phenomenal, supportive boyfriend Devin Wayman for their immense moral support and encouragement throughout my graduate experience.

The completion of my research would not have been possible without the incredible mentorship and expertise of Dr. April Weissmiller, my thesis advisor. I want to thank her for the multitude of hours spent guiding me through experiment techniques, research victories and failures, and the scientific reading and writing processes. I am also deeply appreciative of Dr. Jason Jessen and Dr. Brian Robertson for sitting on my committee, taking time to read my thesis, and encouraging my pursuit of biological knowledge. Additionally, I would like to sincerely thank my fellow students in the Weissmiller Lab and my fellow MTSU graduate students for their wise guidance through the master's program and assistance in the laboratory.

Last but certainly not least, I want to thank the Graduate Scholarship Committee for awarding the Mary C. Dunn Summer Stipend and Thomas Hemmerly Graduate Student Research Scholarship to me, which provided financial support for laboratory supplies and living expenses during Summer 2022 research.

ABSTRACT

Neuroblastoma is a pediatric cancer of the nervous system, and high-risk patients are known to have poor prognoses. N-MYC is an oncoprotein transcription factor that is commonly overexpressed through gene amplification in high-risk pediatric neuroblastoma cases. In order for N-MYC to drive oncogenesis, it must first bind chromatin to regulate expression of target genes linked to cancer functions. The chromatin regulator WDR5 has been shown to directly bind the c-MYC family member and facilitate recruitment of MYC to chromatin at genes involved in cancer-regulated functions such as protein synthesis, cell cycle progression, proliferation, and apoptosis. However, whether this is true for N-MYC in neuroblastoma remains unknown. During my thesis work, we identified a conserved core set of binding sites known to be bound by both N-MYC and WDR5. Then, to investigate the impact of WDR5 on the ability of N-MYC to bind chromatin, multiple approaches to interrupt the N-MYC-WDR5 interaction, such as a dTAG-directed degradation system and a Tet-on inducible genetic system, were used in the engineered neuroblastoma cell lines. Results demonstrate that when N-MYC was unable interact with WDR5, N-MYC binding to chromatin was specifically decreased at sites co-bound by N-MYC and WDR5. Our findings have implications for high-risk neuroblastomas and pave the way for novel treatment avenues involving inhibition of the N-MYC-WDR5 interaction as a new approach to block N-MYC function.

TABLE OF CONTENTS

Introduction.....	1
1. Neuroblastoma.....	1
2. N-MYC.....	3
3. WDR5.....	5
4. N-MYC-WDR5 Interaction.....	7
5. Study Aims and Design.....	10
Materials and Methods.....	15
Results.....	20
Discussion.....	30
References.....	33

LIST OF FIGURES

Figure 1: Model of dTAG-induced degradation of WDR5 in engineered CHP-134 cells.....	11
Figure 2: Three engineered neuroblastoma SHEP cell lines.....	13
Figure 3: Hypothesized model of N-MYC binding to chromatin in each engineered SHEP cell line.....	14
Figure 4: Venn diagram comparing N-MYC chromatin binding sites to WDR5 binding sites to show their overlap.....	21
Figure 5: In an N-MYC-amplified IMR-32 cell line, WDR5 and N-MYC bind at conserved WDR5 sites but not at N-MYC only sites.....	22
Figure 6: FKBP-tagged WDR5 is exclusively expressed in DT-WDR5 CHP-134 cells.....	24
Figure 7: dTAG degradation of WDR5 occurs rapidly over 4 hours and does not impact N-MYC protein levels in CHP-134 cells.....	24
Figure 8: WDR5 degradation reduces N-MYC chromatin binding at conserved WDR5 target genes in CHP-134 cells.....	26
Figure 9: DOX-induced N-MYC expression in WT- and WBM-SHEP is comparable to N-MYC expression in N-MYC amplified cells.....	28

Figure 10: A mutated WBM site reduces the ability of N-MYC to bind chromatin at
WDR5-N-MYC co-bound loci.....29

LIST OF TABLES

Table 1. Human neuroblastoma cell lines used in this study.....	14
Table 2: Primers utilized for all ChIP experiments in this thesis.....	18

INTRODUCTION

1. Neuroblastoma

Neuroblastoma is a rare, cancerous tumor of the sympathetic nervous system that develops only in children, and most children with this cancer are sadly diagnosed before the age of 5. An estimated 800 cases are newly diagnosed per year in the United States, and it is the most common cancer in infants younger than 1 year old (1).

Neuroblastoma develops from abnormal differentiation of fetal nerve cells called neuroblasts. These tumors are most commonly found growing in adrenal glands, but the spine, spinal cord, abdomen, and chest are additional areas that primary or metastatic tumors can form (1). Persistent aches, generalized pain, abdominal distention and pain, abnormal gait, appetite loss, and irritability are symptoms typically experienced in neuroblastoma patients (2). Treatment of both the disease and the symptoms are imperative for newly diagnosed infants and children.

Current common neuroblastoma treatments include surgery, chemotherapy, and radiation, and treatment options vary depending on whether a child is characterized as being low-, intermediate-, or high-risk. Low and intermediate risk children have an optimistic 5-year survival rate of about 95%, but high-risk children have a 5-year survival rate of less than 50% (3). While some patients can achieve hopeful outcomes with conventional therapies listed above, the high-risk population exhibits unfavorable prognoses and relatively less successful treatment responses. High-risk cases of neuroblastoma are described as being aggressive and typically require intensive

treatment with numerous types of therapy, with treatment regimens spanning 18 months on average (4). 10-15% of children with high-risk neuroblastoma who undergo treatment have refractory disease, meaning that the treatment was ineffective against the cancer. Additionally, cancer will return in 40-50% of children with high-risk neuroblastoma, even after their cancer is initially treated by current, extensive treatments (4). High-risk neuroblastoma can be detrimental to young patients and their families; therefore, this high-risk group of patients warrants the ongoing pursuit of novel treatment options.

2. N-MYC

It is known that high-risk neuroblastoma is associated with amplification of the *MYCN* gene, which encodes the N-MYC transcription factor. The MYC family of transcription factors (N-MYC, c-MYC, l-MYC, and v-MYC) are major oncogenes in cancer whose overexpression is observed in more than half of all malignancies and a wide array of different tumor types (5). N-MYC, like any other MYC protein, is a DNA-binding transcription factor capable of regulating transcription of genes involved in proliferation, genome instability, protein synthesis, metabolism, and apoptosis, all of which are integral to cancer formation (6). N-MYC structurally falls under the basic helix-loop-helix-zipper (bHLHZ) class of proteins, and in order to bind chromatin, it must dimerize with another bHLHZ (7) protein called MAX. N-MYC localizes in the nucleus, where any dysregulation of the protein can be developmentally problematic. N-MYC down-regulation or deletion can be lethal to embryos, and up-regulation or amplification can result in tumorigenesis (8).

N-MYC is found primarily in solid tumors of neural origin, and as mentioned above, amplification of *MYCN* at the chromosomal level can be an adverse prognostic factor for high-risk neuroblastoma (5). The two most common ways MYC activity is impacted are 1) changes to *MYC* loci that stimulate increased MYC transcription, or 2) extrinsic to MYC that impact regulatory mechanisms (6). In neuroblastoma, amplification of MYC proteins can occur via duplications of the *MYC* oncogene in the same chromosome, known as homogeneously staining regions, or in extrachromosomal

duplications of *MYC* called double minutes. Up to 800 copies of the *MYCN* gene have been recorded in some tumor cells (9). This amplification can induce oncogenic qualities early in human development.

The most direct route to targeting N-MYC is to block its ability to bind chromatin and subsequently transcribe genes, but MYC proteins generally, like many transcription factors, are largely unstructured in the absence of partner proteins and therefore has been difficult to target directly. Because MYC is unstructured and cannot bind DNA by itself, it must heterodimerize with its obligate binding partner MAX to recognize target DNA sequences called e-boxes that are located across the genome (10). As it pertains to N-MYC in N-MYC amplified neuroblastoma, targeting N-MYC directly has remained a challenge, and no small molecules have been discovered that can directly inhibit N-MYC because of its lack of defined structure. Additionally, N-MYC is shaped similarly to all MYC family proteins, making it difficult to exclusively target N-MYC without targeting other MYC proteins and impacting their healthy functions (10). Because N-MYC interacts with numerous nuclear proteins during its role as an oncogenic transcription factor and requires dimerization with another bHLHZ protein to bind chromatin (7), researching N-MYC as an anti-cancer target can be complex and involves investigating the interactions between N-MYC and its various binding partners.

3. WDR5

WD repeat-containing protein 5 (WDR5) is known to drive healthy human development through its interactions with multiple interaction partners. One of the first discovered roles of WDR5, found in osteoblasts and odontoblasts, was its promotion of bone formation and cellular differentiation, where WDR5 overexpression resulted in an abnormally large skeleton (11). In another study, WDR5 depletion resulted in developmental defects in *Xenopus* embryos due to a subsequent decrease in transcription of *HOX* genes, which are essential for healthy development of body segments (12). WDR5 also plays a significant role in cell division by localizing at mitotic spindles and ensuring stability of microtubules to maintain the integrity of mitosis (13). Additionally, WDR5 is involved in triple-negative breast cancer metastasis (14) and cell proliferation in prostate cancer when overexpressed (15). These data suggest that if WDR5 levels become dysregulated, there can be damaging and even cancerous effects.

It is clear, based on all the described functions of WDR5 above, that WDR5 is a versatile protein involved in multiple cellular functions and is known to interact with a wide array of proteins to perform its functions. Structurally, WDR5 is a β -propeller protein containing 7 blades, with each blade being a set of ~40 amino acids beginning with glycine-histidine (GH) and ending with tryptophan-aspartic acid (WD) (13, 16). Its interactions with partner proteins have been mapped exclusively to either a hydrophobic cleft on its surface called the “WDR5-binding motif” (WBM) or another one of its surface cavities called the “WDR5-interacting” (Win) site, which binds a conserved

arginine motif present on Win-interaction partners. WDR5 is immensely conserved across a multitude of organisms, especially vertebrates, where over 90% of the *WDR5* sequence is identical across various vertebrate species (13). In mammalian cells, the canonical role of WDR5 is as a core scaffolding subunit of several histone methyltransferase complexes, propelling assembly of chromatin modifying complexes in the nucleus (17). Although histone modification is the canonical role of WDR5, this versatile protein also plays significant roles in additional, non-canonical cellular processes outside of the nucleus. In 2015, a new role for WDR5 was discovered in that WDR5 can interact directly with the c-MYC family member through a conserved set of amino acids present in all MYC family members (18), adding to the list of known WDR5 functions and opening up the possibility that WDR5 may influence the function of a major oncogene in cancer. Therefore, because of its involvement in various cancerous tumor types and its known interaction with MYC (18), investigation of WDR5 in the context of neuroblastoma is warranted to determine if the N-MYC-WDR5 protein interaction can serve as an anti-cancer approach.

4. The MYC-WDR5 Interaction

The basic mechanism by which a MYC protein will promote cancer processes is by binding near genes that it can regulate. One critical co-factor that is known to influence the ability of MYC to bind to its target genes is WDR5, which binds c-MYC directly within a region of all MYC proteins known as the Myc box III (18). While, as mentioned, WDR5 itself is a protein that is involved in a variety of cellular processes, including cell cycle progression, signal transduction, apoptosis, and gene regulation (16), it is thought that these various additional processes are separate from the role it possesses when in complex with MYC. As it relates to the MYC-WDR5 interaction, it has been shown that WDR5 interacts with c-MYC to regulate the ability of c-MYC to bind genes in the context of chromatin (18, 19). Mutation of the WDR5-binding motif (WBM) within Myc box III of c-MYC can disrupt the interaction of c-MYC with WDR5 and cause a reduction in c-MYC binding at specific genes overwhelmingly linked to protein synthesis functions (6, 18). Furthermore, it was demonstrated that in Burkitt's lymphoma, which is a cancer driven by translocation of c-MYC to a high-expressing IgH locus, that disrupting the interaction of MYC-WDR5 promotes tumor regression as effectively as completely preventing MYC from binding DNA (19), indicating that the MYC-WDR5 interaction is essential for tumor maintenance. These data have led to the idea that c-MYC is recruited by WDR5 to multiple genes believed to have significant impact on tumor formation and survival (19). Together these data suggest that perturbing the MYC-

WDR5 interaction could lead to reduced binding of MYC to chromatin and subsequent antitumorigenic effects.

The discovery that WDR5 can impact numerous aspects of MYC function illuminates the possibility that the MYC-WDR5 interaction can serve as a focal point for new therapeutic approaches to target MYC. In terms of inhibiting N-MYC in neuroblastoma, a direct and targeted N-MYC therapy would be regarded as a sought-after approach, but as mentioned, due to the unstructured shape of MYC, no direct therapies have been discovered (10). If WDR5, which has a well-folded structure and therefore is more amenable to small molecule inhibition (20), can be targeted instead, then there is potential that MYC function can be affected as well. For patients with N-MYC amplified neuroblastoma, this could result in one of the first N-MYC targeted approaches, which is much needed for these devastating pediatric cancers. However, to fully understand how broadly the MYC-WDR5 nexus can be utilized as a focal point for any novel therapy ideas, it is critical to understand the impact of WDR5 on MYC in other cancer contexts beyond Burkitt's lymphoma, such as neuroblastoma.

My thesis work lies in understanding the degree by which WDR5 can influence a fundamental function of N-MYC, which is to bind target genes. Given that N-MYC, like any MYC protein, must bind chromatin in order to activate transcription, focusing on this process will be essential in understanding any functional impact that results from inhibiting the N-MYC-WDR5 interaction in future studies. Therefore, in neuroblastoma,

the hypothesized recruitment of N-MYC to chromatin by WDR5 serves as a sensible avenue to explore for anti-cancer therapy research.

5. Study Aims and Design

Based on the combination of published data described above and preliminary data present in the Weissmiller laboratory, I hypothesized that blocking the interaction of N-MYC with WDR5 would cause a reduction in N-MYC binding to chromatin at specific subsets of N-MYC target genes. I tested this hypothesis by first identifying a set of genomic loci that are conserved in N-MYC amplified cell lines, and then secondly, investigating whether blocking the interaction of N-MYC with WDR5 does impact N-MYC binding. These experiments were performed on a gene-by-gene basis using chromatin immunoprecipitation (ChIP) and quantitative polymerase chain reaction (QPCR) at select loci predicted to be WDR5 binding site targets. Different neuroblastoma cell lines are heterogenous and are known to possess differing idiosyncratic characteristics (21). Because of this, my research was conducted across three human neuroblastoma cell lines: CHP-134, IMR-32, and SHEP (Table 1), to further demonstrate whether the relationship between N-MYC and WDR5 is significant in the context of neuroblastoma.

The three cell lines used in this experiment possess unique qualities. Firstly, IMR-32 cells are N-MYC amplified, derived from a 13-month-old male patient's abdominal tumor. Secondly, CHP-134 cells are N-MYC amplified and derived from an 18-month-old male patient's primary adrenal gland tumor. These two cell lines were used to examine the extent of N-MYC and WDR5 binding in N-MYC amplified cell lines and provided the set of conserved binding sites that I could use to assess the impact of WDR5 on N-MYC binding to chromatin. As a first approach, CHP-134 cells were engineered so that the

only form of endogenous WDR5 they expressed carried a FKBP(F36V)-tagged version of WDR5 that can be degraded by small molecule dTAG administration via linking WDR5 to an E3 ubiquitin ligase complex and promoting subsequent proteasome-mediated degradation (Figure 1) (22). The dTAG degradation system is an appropriate method to reduce WDR5 because addition of a dTAG molecule can induce rapid changes in protein levels through acute depletion of the target protein (22).

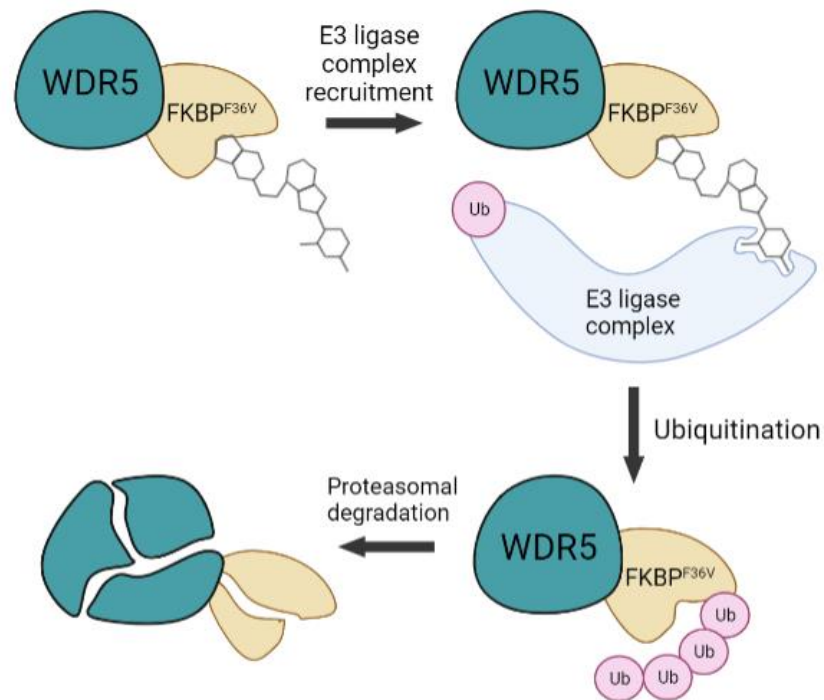


Figure 1: Model of dTAG-induced degradation of WDR5 in engineered CHP-134 cells. WDR5 is expressed with a small portion of the FKBP protein containing a mutation (F36V) which can allow binding of the dTAG molecule. dTAG molecules fuse WDR5-FKBP^{F36V} with an E3 ligase complex, which ubiquitinates WDR5 and routes it for proteasomal degradation. Ub is ubiquitin. Image created with BioRender.

As a second approach, SHEP cells, which are derived from a 4-year-old female patient's bone marrow metastasis tissue but have been cloned out so that they do not possess malignant characteristics (23) nor express N-MYC, were engineered to genetically induce N-MYC expression via doxycycline administration using the Tet-on system. As shown in Figure 2, the Tet-on system utilizes administration of a tetracycline derivative, doxycycline, to express, in our case, either wild-type N-MYC (WT-N-MYC, WT-SHEP), a version of N-MYC that is unable to bind WDR5 (WBM-N-MYC, WBM-SHEP), or green fluorescent protein (GFP) as a control (GFP-SHEP). This inducible system provides an avenue to control N-MYC expression in the SHEP cells. Because N-MYC is not constitutively or endogenously expressed in SHEP cell lines, we can use these cells to model how the ability of N-MYC to bind chromatin is impacted by blocking the N-MYC-WDR5 interaction in the WBM-SHEP cells. As an illustration to our hypothesis for these cell lines, there should be no N-MYC present in the GFP-SHEP cells while N-MYC should be bound normally to chromatin in WT-SHEP cells. Then, if the N-MYC-WDR5 interaction is important for facilitating N-MYC binding to chromatin, N-MYC should not be bound to chromatin in the WBM-SHEP cell line (Figure 3). In summary, two separate approaches were utilized to investigate the hypothesis, and the results are presented in this thesis.

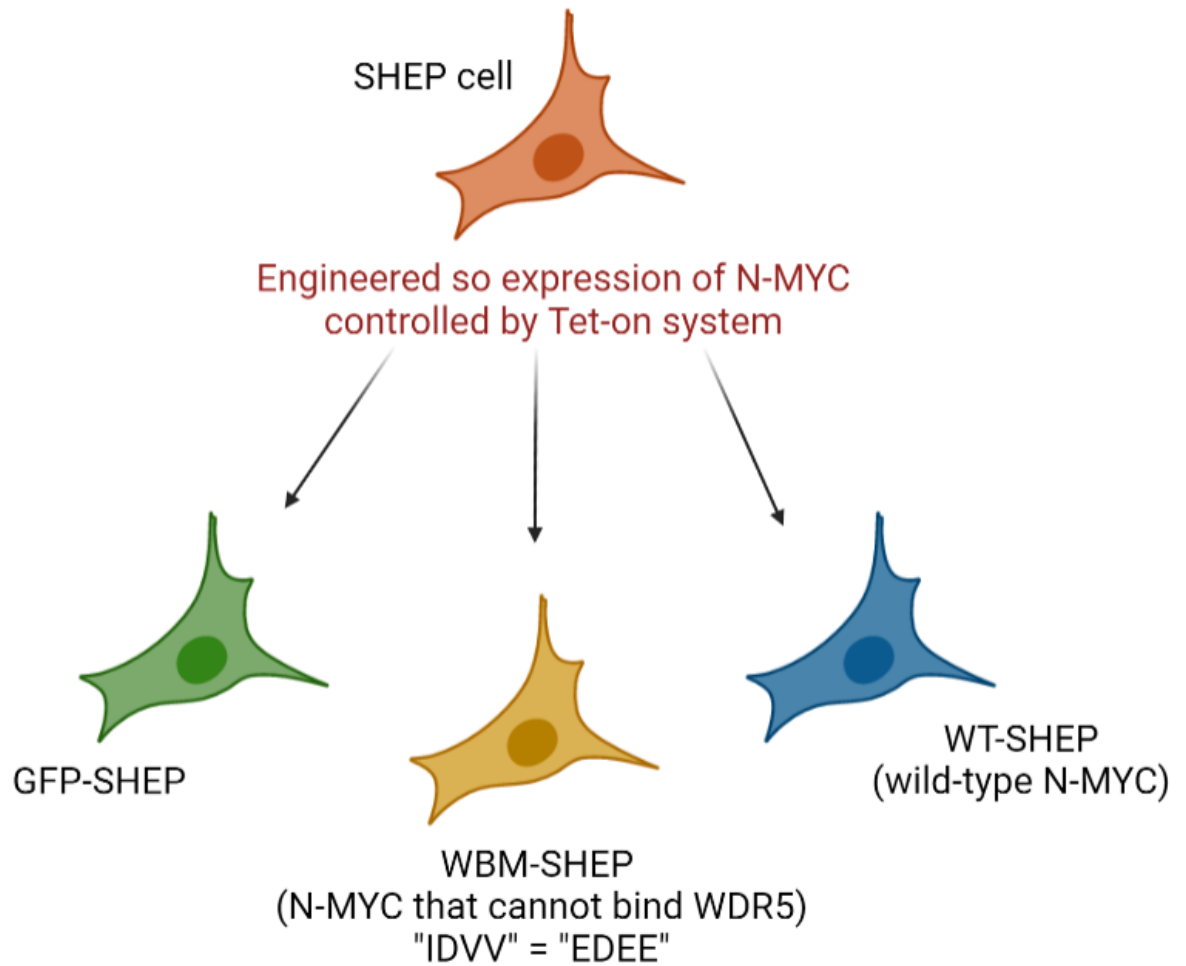


Figure 2: Three engineered neuroblastoma SHEP cell lines. GFP-SHEP is the negative control line. WBM-SHEP is the experimental line. It contains a mutation to the domain of N-MYC that binds WDR5 which renders the proteins unable to bind. WT-SHEP expresses the wild-type N-MYC protein containing no mutations. Model created with BioRender.

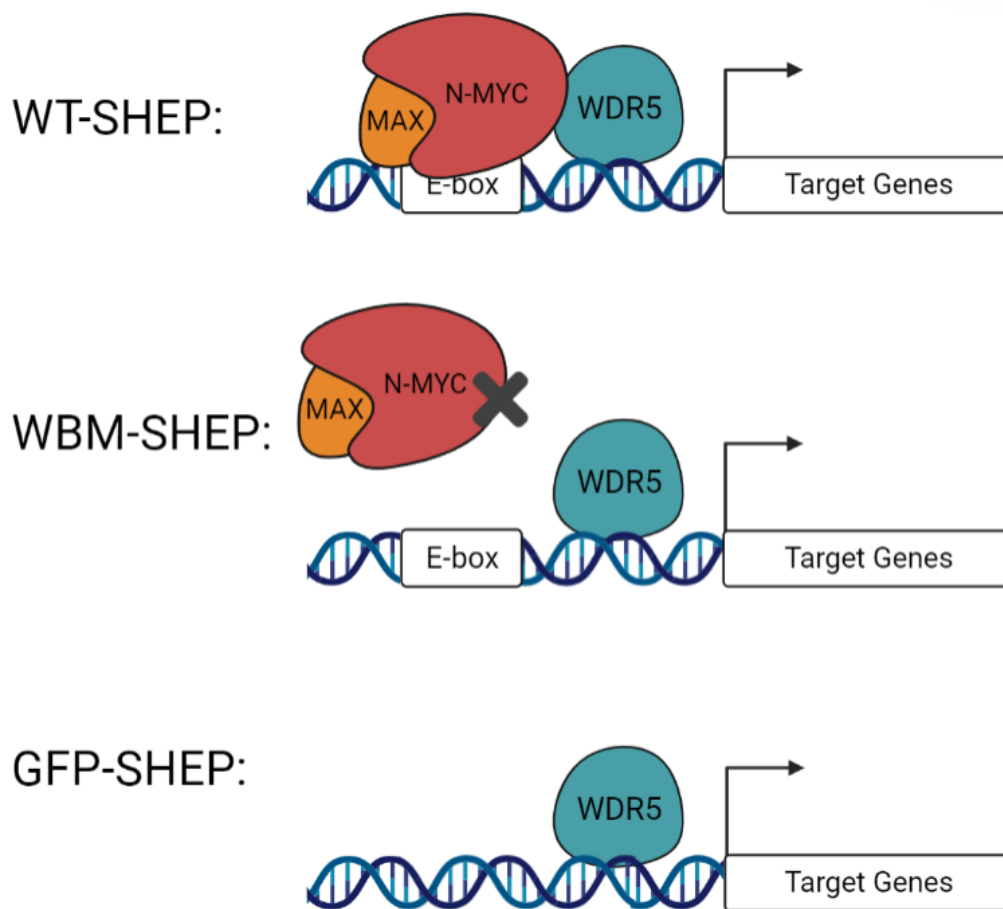


Figure 3: Hypothesized model of N-MYC binding to chromatin in each engineered SHEP cell line. WDR5 is hypothesized to bind N-MYC and recruit it to chromatin in cells expressing wild-type N-MYC (WT-SHEP) cells. In the WBM-SHEP cell line, it is hypothesized that reduced N-MYC recruitment to chromatin will occur due to these cells expressing a version of N-MYC with a mutation in the WDR5-binding motif (WBM site). GFP-SHEP is our negative control cell line that should not endogenously express N-MYC but should show induced green fluorescent protein expression. Downstream transcriptional rates were not measured in this thesis. Model created with BioRender.

Cell line	Primary or Metastasis	Tissue derived from	N-MYC status
CHP-134	Primary	Adrenal gland	Amplification
IMR-32	Metastasis	Abdominal mass	Amplification
SHEP	Metastasis	Bone marrow	Non-amplified; no endogenous N-MYC

Table 1. Human neuroblastoma cell lines used in this study.

MATERIALS AND METHODS

Cell lines and cell culture

Engineering of non-N-MYC amplified SHEP cells and N-MYC amplified CHP-134 cells was completed prior to the initiation of this project. SHEP cells were engineered to express a Tet-inducible version of wild-type N-MYC (WT-SHEP), a version of N-MYC that cannot bind to WDR5 (WBM-SHEP), or green fluorescent protein (GFP-SHEP) as a control. For engineered CHP-134 cells (DT-WDR5 CHP-134), the endogenous locus of WDR5 in these cells was previously engineered via CRISPR/Cas9 technology (20, 24) so that endogenous WDR5 is expressed with an in-frame FKBP(F36V) tag which can target WDR5 for rapid proteolysis through the dTAG approach (22). Parental SHEP cells and the N-MYC amplified IMR-32 cell line were provided by Dr. Dai Chung at UT Southwestern. Parental CHP-134 cells used for engineering were purchased from Sigma. All cell lines described in this thesis were maintained in RPMI 1640 1x with L-glutamine media (Corning), supplemented with 1% Gibco Penicillin-Streptomycin (10,000 U/mL) and 10% fetal bovine serum (FBS). For engineered SHEP cells, normal FBS was replaced with tetracycline system-approved FBS (Takara Bio). All cells were grown in a 37°C incubator with 5% carbon dioxide.

Chromatin Immunoprecipitation (ChIP)

To generate chromatin, approximately 1.0×10^7 Tet-inducible SHEP cells were induced with 1 $\mu\text{g}/\text{mL}$ doxycycline (Sigma-Aldrich) 24 hours before chromatin extraction

(Figure 9) to allow for protein expression. Cells were fixed with 1% formaldehyde (Fisher Scientific) for DNA-protein crosslinking for 10 minutes, collected, and nuclei extracted using nuclear extraction buffer (10 mM HEPES [pH 7.9], 10 mM KCl, 100 μ M EDTA, 0.4% NP-40). Nuclear pellets were lysed with FALB (50 mM HEPES [pH 7.5], 140 mM NaCl, 1 mM EDTA, 1% Triton) with 1% SDS. Cells were sonicated using the Diagenode Bioruptor Plus in Bioruptor-compatible 1.5 ml tubes in cycles of 30 seconds on followed by 30 seconds off for extraction of chromatin for a total of 25-35 minutes. Cell passage number was noted for every sample. For DT-WDR5 CHP-134 cells, 1.0×10^7 cells were treated with 500 nM dTAG47 molecule or matched dimethyl sulfoxide (DMSO) in their maintenance media for 4 hours prior to chromatin extraction following same protocol described. IMR-32 cells were untreated, and approximately 7.5×10^6 cells were collected per sample for chromatin using same procedure. All chromatin was aliquoted and stored at -80°C until ChIP was performed.

For the ChIP, approximately 1.0×10^7 cells were used per sample. During set-up, one input tube per sample was created for all cell lines containing 1/50th the amount of the chromatin for normalization and placed in 20°C storage. ChIP was performed overnight at 4°C on the chromatin samples for cell lines using an antibody targeted against N-MYC (Cell Signaling Technology Rabbit mAb, 51705S), WDR5 (Rabbit mAb Cell Signaling Technology, 8884S), or a matched IgG control (Normal Rabbit IgG Cell Signaling Technology, 2729S). The next day, Protein A agarose beads (Thermo Fisher) were blocked with 1% bovine serum albumin, added to tubes, and chromatin samples were

rotated together at 4°C for three hours. Samples and inputs were washed with low salt buffer (20 mM Tris, 150 mM NaCl, 2 mM EDTA, 1% Triton), high salt buffer (20 mM Tris [pH 8.0], 500 mM NaCl, 2 mM EDTA, 1% Triton), Lithium Chloride buffer (10 mM Tris [pH 8.0], 25 mM LiCl, 1 mM EDTA, 1% Triton), and twice with 1X Tris-EDTA (TE) buffer (10 mM Tris [pH 8.0], 1 mM EDTA). Each wash was 5 minutes. 1µl proteinase K (Fisher Scientific) was added to each sample and placed in a 65°C water bath for DNA-protein decrosslinking overnight. All samples were diluted with 1X TE and stored at 20°C until ready for subsequent quantitative polymerase chain reaction (QPCR).

QPCR

QPCR on an Agilent AriaMx Real-Time PCR System was used to analyze DNA fragments that were co-immunoprecipitated with proteins. Samples were set up in triplicate on a 96-well plate. Each well contained 7.5 µl 2X Perfecta SYBR (QuantaBio, 101414-272), 0.9 µl 5uM Forward Primer, 0.9 µl 5uM Reverse Primer, 2.0 µl DNA from sample, and 3.7 µl nuclease-free water (Fisher Scientific). The primers we utilized amplify an 80-100 base pair amplicon length for each loci examined. Primer sequences are provided in Table 1 below. We normalize the amount of immunoprecipitated DNA to input (using $100(2^{((\text{input Cq average} - 5.6) - \text{ChIP Cq average}))})$) when analyzing the data, and graphs of our results are generated on Prism GraphPad software.

Name	Forward Sequence	Reverse Sequence	Predicted use
SNHG15	CGCCACTGAACCCAATCC	TCTAGTCATCCACCGCCATC	Conserved WDR5
EIF4G3	CCTTTCACGGCAATATCCTC	TGAGTGAAGAAAATCCACCG	Conserved WDR5
RNPS1	GATGTAAGTTGGGGCGGAAT	GAGGAGTGGACCGGCTTC	Conserved WDR5
RPS6	GAGACCTTCTCCACCTAAA	CGAGTGTTAGACTGGGTTTG	Conserved WDR5
CCT7	TTCCAAAATGATGGTGAGTG	AGAGGGTCTACAGAGCAAG	Conserved WDR5
RPL35	CTTGTGCAGCAATGGTGAGA	GCCTAGGTGGCAGATAGAATC	Conserved WDR5
RPL17	CAGCGAGGATTTAGTAGCC	GTTTCTCCTGCGTTGCTC	Conserved WDR5
METTL1	GCATGGCTGCGTCATTAAT	GAGTCTCGGCTGCCATGAT	N-MYC only
SURF6	GGGTGATAGAGGCACTGAGG	GATTAGCCAAGCCTGACTCC	N-MYC only
RPL10	GCAAGAGTTCTACGCCAAG	CACATGCCGAGATCAGAGAG	N-MYC only
RPS12	TCTGAAGACTGCCCTCATCC	CTTGGGTGGCAGTTTTGTTC	N-MYC only
BGLO	GGCTGTCATCACTTAGACCTC	GGTTGCTAGTGAACACAGTTG	Negative control locus

Table 2: Primers utilized for all ChIP experiments in this thesis.

Protein Lysates

Cells were washed with 1X phosphate-buffered saline (PBS). 1% Triton lysis buffer (25 ml 1M Tris [pH 8.0], 15 ml 5 M NaCl, 5 ml 0.5 M EDTA, 50 ml 10% Triton [Fisher Scientific]), supplemented with protease inhibitors [Sigma Aldrich], and 0.1 M PMSF [Tocris Bioscience]) were added to each sample. Cells were lysed via sonication for 15 seconds on 25% power and debris cleared through centrifugation at 13,000 R.P.M. for 10 minutes at 4°C. A fraction of the soluble proteins were added to Protein Assay Dye (BioRad) and transferred to cuvettes. A spectrophotometer set at 595 nm wavelength was used to measure absorbance values of each sample, and samples were normalized to each other to make them have equal concentrations. Then, SDS loading

dye was added to each tube, and samples were boiled at 95°C for 5 minutes. All samples were stored at -20°C until future processing.

Western Blotting

Protein lysate samples were resolved on an SDS-PAGE gel and transferred to PVDF membrane (Fisher Scientific). PVDF membrane was soaked in 100% methanol for 5 minutes then soaked in 1X Transfer buffer containing 10% methanol. All resolved proteins were transferred to the PVDF membrane overnight at 25V at 4°C. PVDF membrane was removed and soaked in BLOCK solution (5% dry milk powder in TBS-T [0.1% Tween]) for 1 hour on shaker at room temperature prior to addition of antibodies. The Anti-N-MYC Rabbit mAb, Anti-GAPDH Rabbit mAb, and the Anti-WDR5 Rabbit mAb were from Cell Signaling (51705S, 8884S, and 13105S, respectively). Membranes were washed extensively in TBS-T and developed using chemiluminescence substrate (BioRad). Blots were imaged using the chemiluminescence imaging application on a ChemiDocMP Imaging System (BioRad).

RESULTS

N-MYC and WDR5 co-localization in N-MYC amplified neuroblastoma cell lines.

To begin to gain insight into how WDR5 may influence N-MYC function, we first investigated the chromatin-binding properties of N-MYC and WDR5 in the N-MYC amplified cell line called CHP-134, which is derived from an 18-month-old male patient's adrenal tumor. Genome-wide chromatin binding data collected through performing chromatin immunoprecipitation coupled to next-generation sequencing (ChIP-seq) show that N-MYC was detected at over 10,000 sites in the genome and that WDR5 was detected at ~1,500 sites. Overlap of their binding sites reveals that 87% of WDR5-bound sites are found co-localized with N-MYC (Figure 4), indicating that N-MYC and WDR5 may interact with each other at these sites. Because neuroblastomas are heterogenous in nature, it is imperative to confirm that N-MYC and WDR5 co-localize at at least some of these sites consistently across different cell lines of various origins. Therefore, we assessed N-MYC and WDR5 chromatin binding on a gene-by-gene basis in the cell line called IMR-32, which is derived from a metastatic abdominal mass in a 13-month-old male patient. The genes we chose to examine for co-localization were chosen from the ~1,400 overlapped sites detected in CHP-134 cells (Figure 4) and are also among the 94 conserved and context-independent sites that have been published for WDR5 (20). Using quantitative polymerase chain reaction (QPCR), we probed 11 loci involved in various functions such as protein synthesis, proliferation, and cell cycle. Results confirm that N-MYC and WDR5 bind at these specific conserved sites (Figure 5). As expected, N-

MYC can also bind chromatin without WDR5, which is in line with the ability of N-MYC to bind to many other locations across the genome that do not overlap with WDR5 (Figure 4, left side of Venn Diagram). Taken together, N-MYC and WDR5 co-localize at an abundant number of genomic sites, which in addition to the high-confidence list of 94 conserved WDR5 sites detailed by Bryan et. al (20), provides us numerous loci at which to ascertain the impact of WDR5 on the ability of N-MYC to bind chromatin.

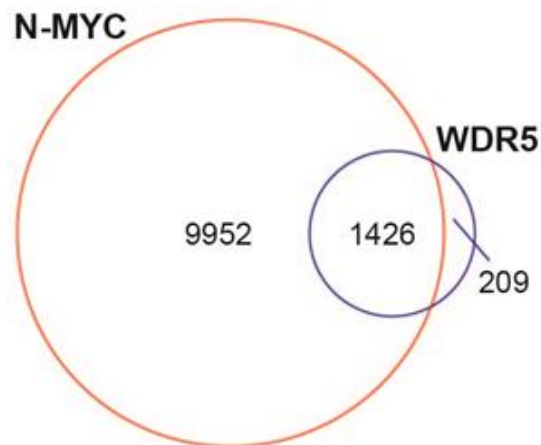


Figure 4: Venn diagram comparing N-MYC chromatin binding sites to WDR5 binding sites to show their overlap. Data obtained from ChIP-seq analysis of N-MYC amplified CHP-134 cells. WDR5 is found co-localized with N-MYC at 87% of WDR5 target genes (1,426 genes).

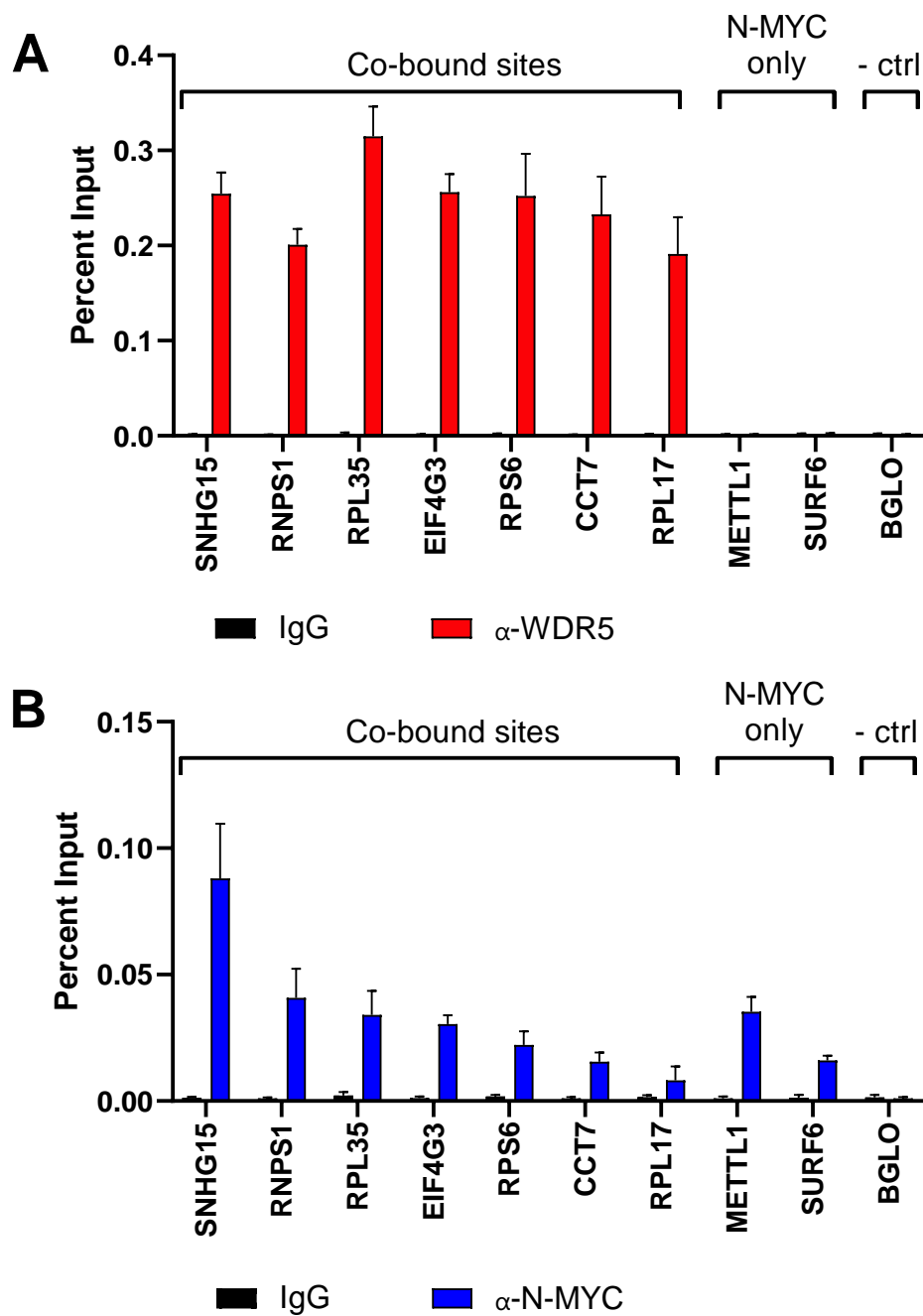


Figure 5: In an N-MYC-amplified IMR-32 cell line, WDR5 and N-MYC bind at conserved WDR5 sites but not at N-MYC only sites. **A.** WDR5 binds only at conserved WDR5 sites. **B.** N-MYC binds at conserved WDR5 sites and N-MYC only sites. Amount of immunoprecipitated DNA was normalized to input DNA and percent input calculated and graphed. BGLO is a negative control locus. Graph created in Prism GraphPad software.

A dTAG system to study the effect of depleting WDR5 on the ability of N-MYC to bind chromatin.

Next, we determined if we could measure the influence of WDR5 on the ability of N-MYC to bind chromatin in N-MYC amplified cells. We know that N-MYC and WDR5 co-localize at numerous genes, and we want to explore whether the absence of WDR5 would impact N-MYC recruitment to chromatin. Subsequently, we took advantage of the dTAG degradation method that has recently been characterized (22) and used actively in this lab (25). CHP-134 cells were engineered so that the sole form of WDR5 in the cells contains a FKBP-degron tag that would allow WDR5 to be degraded by the addition of a small molecule dTAG47 degrader (20, 24). Figure 6 shows a western blot confirming that the only form of WDR5 present in the engineered cells (called DT-WDR5 CHP-134 in this thesis) was the FKBP-tagged version, which produced a size shift on the western blot to a higher size than endogenous WDR5. In these cells, adding 500nM of dTAG47 provides a rapid method to diminish target protein levels (20, 22, 24). However, we first had to perform a time course experiment to ascertain the duration required for optimal WDR5 degradation. Results of this time course confirmed that 500nM dTAG47 induces full degradation of WDR5 within 4 hours of administration, when compared to a dimethyl sulfoxide (DMSO) vehicle control. Importantly, treatment of cells with dTAG47 did not impact N-MYC protein levels (Figure 7).

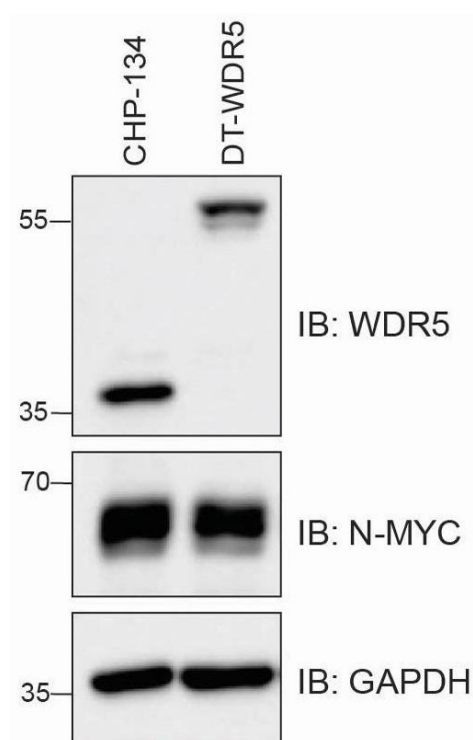


Figure 6: FKBP-tagged WDR5 is exclusively expressed in DT-WDR5 CHP-134 cells. Western blot demonstrating that the 56 kDa version of FKBP-tagged WDR5 is the only version of WDR5 present in DT-WDR5 CHP-134 cells. Untagged WDR5 is 37 kDa, none of which is present in DT-WDR5 cells. Tagged WDR5 does not affect N-MYC protein levels. GAPDH is shown as a loading control. "IB" stands for "immunoblot" and indicates the antibody used.

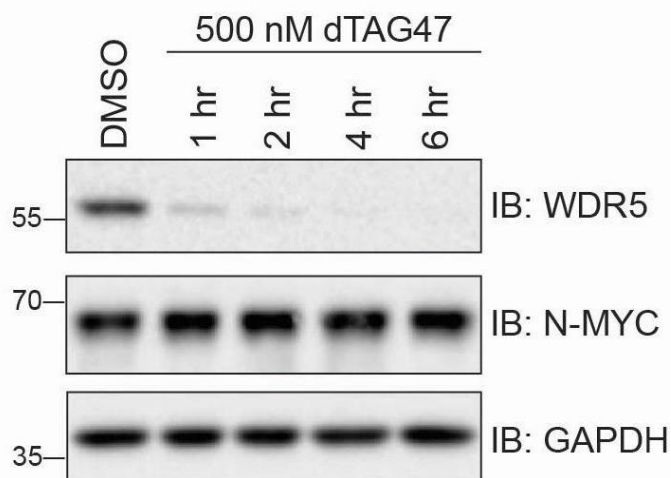


Figure 7: dTAG degradation of WDR5 occurs rapidly over 4 hours and does not impact N-MYC protein levels in CHP-134 cells. The 4-hour post-dTAG47 administration timepoint represents the optimal time for full WDR5 degradation. Degradation of WDR5 does not affect N-MYC protein levels at any 1-6hr timepoint. At the 4-hr timepoint in which N-MYC/WDR5 binding was analyzed via QPCR (Figure 9), WDR5 was completely degraded.

To probe the impact of WDR5 degradation on the ability of N-MYC to bind chromatin, DT-WDR5 CHP-134 cells were treated with either DMSO (vehicle control) or dTAG47 over 4 hours. Chromatin was extracted, sonicated, and immunoprecipitated using antibodies targeted against WDR5, N-MYC, or IgG as a control. QPCR analysis using our defined set of genomic sites from Figure 5 was conducted with each sample to indicate the amount of signal detected for IgG, WDR5, and N-MYC at WDR5 target and non-WDR5 target loci. Results reveal that in cells treated with dTAG47, as expected, WDR5 no longer binds chromatin when compared to the signal detected for WDR5 in DMSO control-treated cells (Figure 8), indicating that dTAG47 successfully degrades WDR5 both at the protein level (Figure 7) and the chromatin level (Figure 8). Interestingly, the signal for N-MYC detected at sites of WDR5 loss is reduced, while the signal for N-MYC at non-conserved WDR5 target sites remains very similar regardless of dTAG47 treatment. This indicates that at co-localized sites, WDR5 can play a role in recruitment of N-MYC to chromatin. Overall, WDR5 degradation does appear to impact the ability of N-MYC to bind chromatin in N-MYC amplified CHP-134 neuroblastoma cells, suggesting that, as has been seen in lymphoma for c-MYC (19), WDR5 can facilitate at least some recruitment of N-MYC to chromatin.

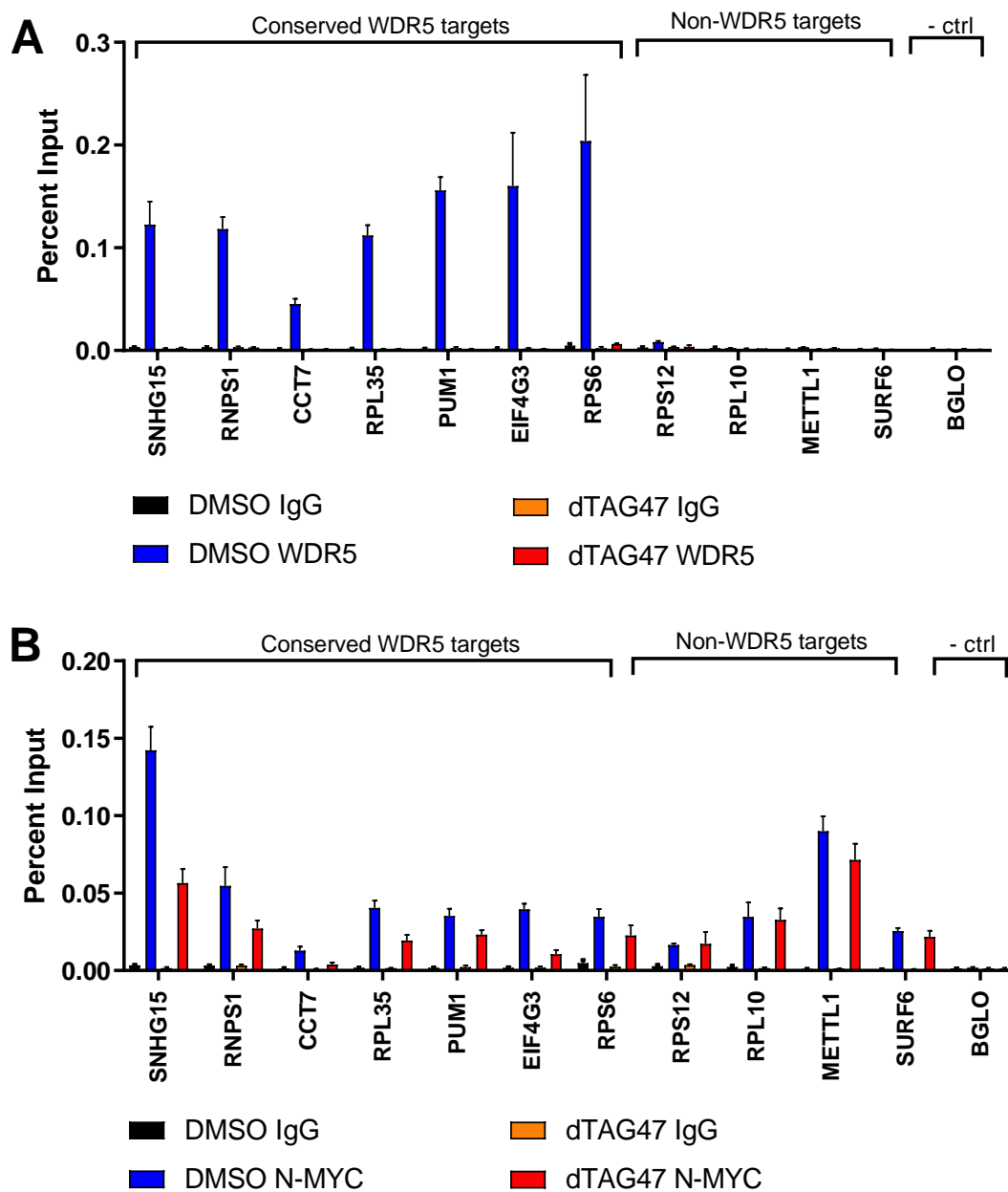


Figure 8: WDR5 degradation reduces N-MYC chromatin binding at conserved WDR5 target genes in CHP-134 cells. **A.** dTAG successfully degrades WDR5, and WDR5 is bound to chromatin in DMSO control cells at the usual conserved WDR5 target loci. **B.** N-MYC binding is not impacted at non-WDR5 target genes, but WDR5 degradation reduces N-MYC binding at conserved WDR5 genes. Chromatin was extracted 4 hours post-dTAG47 administration. IgG is used as a negative control for the antibody. DMSO is the vehicle control. BGLO is used as a negative control locus. Graph created in Prism GraphPad software.

An inducible cell system to study the effect of blocking the N-MYC-WDR5 interaction on the ability of N-MYC to bind chromatin.

Removing WDR5 through the dTAG approach is a rapid method to deplete WDR5 from cells; however, WDR5 has been shown to be important for multiple cellular functions (13) so removing total levels of WDR5 may lead to additional effects that impact N-MYC functions. Therefore, a more direct approach to assess the influence of WDR5 on the ability of N-MYC to bind chromatin may be more desired. As a second approach, therefore, we utilized neuroblastoma SHEP cells, which contain no endogenous N-MYC and are derived from a 4-year-old female patient's bone marrow metastasis. SHEP cells are widely used in the neuroblastoma field to model N-MYC function. Using this system, we could directly and specifically impair the N-MYC-WDR5 interaction by mutating the WDR5-binding (WBM) site within N-MYC, leaving the remaining N-MYC interactions, and WDR5 itself, unperturbed. In addition, we took advantage of the Tet-on system to allow control of N-MYC expression. SHEP cells were engineered to express wild-type N-MYC (WT-N-MYC, WT-SHEP), a version of N-MYC that cannot bind WDR5 (WBM-N-MYC, WBM-SHEP), or green fluorescent protein (GFP) as a control (GFP-SHEP) following addition of a tetracycline derivative, doxycycline (DOX). We utilized DOX because it is known to be less cytotoxic and more stable than tetracycline (26). WBM-SHEP is our experimental cell line containing N-MYC with a mutated WDR5 binding motif (I262E/V264E/V265E, so "IDVV" was engineered to "EDEE" within the total 4 amino acid WBM protein sequence) (19), preventing N-MYC

from binding WDR5. As shown in Figure 9, 24-hour treatment with 1 $\mu\text{g}/\text{mL}$ doxycycline demonstrates that, once induced for 24 hours, the WT and WBM-SHEP cells express N-MYC at comparable levels to the N-MYC amplified CHP-134 and Be(2)C cell line, while the GFP cell line lacks N-MYC expression.

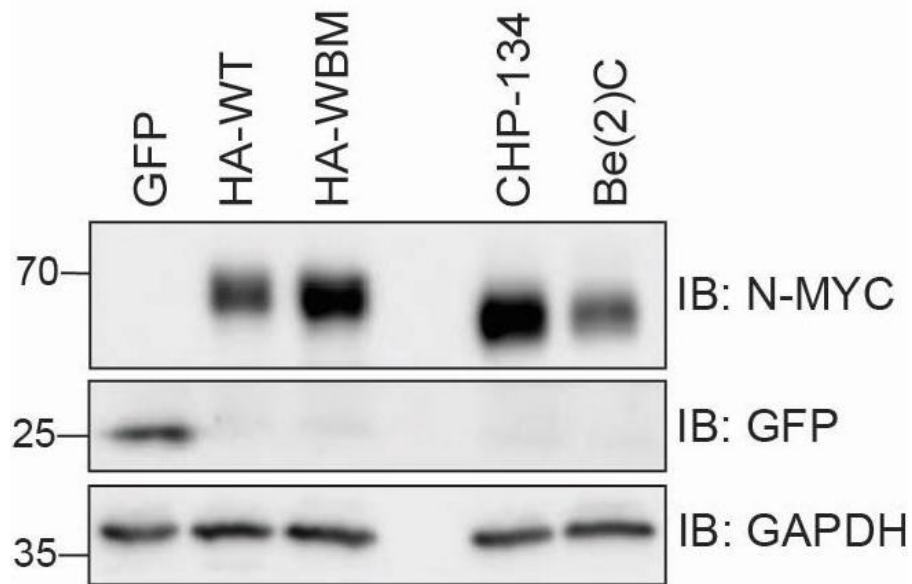


Figure 9: DOX-induced N-MYC expression in WT- and WBM-SHEP is comparable to N-MYC expression in N-MYC amplified cells. Western blot performed at 24 hours post-doxycycline induction. N-MYC expression in the SHEP cell lines (HA-N-MYC and HA-WBM) is comparable to N-MYC expression in N-MYC amplified cell lines CHP-134 and Be(2)C. GFP does not express N-MYC. GAPDH used as a loading control.

Each of the three SHEP cell lines were then induced and subjected to chromatin immunoprecipitation using an antibody against N-MYC and subsequent QPCR analysis with defined sets of loci to examine from above. Results reveal that at conserved WDR5-bound sites, blocking the ability of N-MYC to directly bind WDR5 resulted in a dramatic reduction in N-MYC binding (Figure 10, compare WBM- to WT-SHEP N-MYC signal) while N-MYC binding at non-WDR5 sites was not impacted by the mutation. Collectively, these

data demonstrate that directly disrupting the N-MYC-WDR5 interaction is sufficient to prevent recruitment of N-MYC to chromatin at sites which WDR5 is known to bind regardless of cellular context (20).

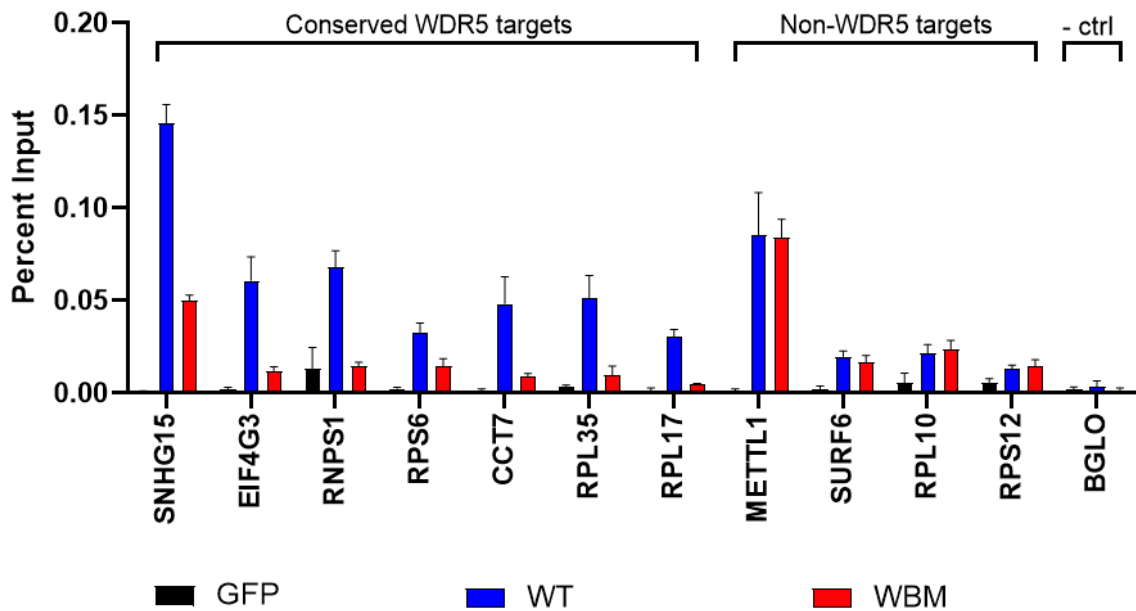


Figure 10: A mutated WBM site reduces the ability of N-MYC to bind chromatin at WDR5-N-MYC co-bound loci. Chromatin was extracted from SHEP cells 24 hours post-doxycycline (1 ug/mL) induction and subjected to ChIP using an antibody against N-MYC. Amount of immunoprecipitated DNA was normalized to input DNA and percent input calculated and graphed. BGLO is a negative control locus, as it is a gene that neither N-MYC or WDR5 are known to bind. Graph generated on Prism GraphPad software.

DISCUSSION

Discovery of novel strategies to combat high-risk pediatric neuroblastoma is a pressing need in the field of oncology. Although N-MYC overexpression correlates with high-risk neuroblastomas, and blocking N-MYC function is accepted as an optimal approach to halting neuroblastoma function, its shape and lack of structure has caused N-MYC not to be amenable to pharmacological targeting (10). Complete knock-out of N-MYC would be too difficult in cancers with N-MYC amplification, especially with some patients reaching up to 800 copies of *MYCN* in their tumor genome (9). Additionally, regulated levels of N-MYC activity are required for healthy fetal and childhood development, so N-MYC reduction in amplified cells may be better than complete N-MYC knock-out (28 Beltran 2014 8). Because of these various issues, targeting N-MYC by focusing on N-MYC interaction partners has surfaced as a promising strategy to block N-MYC functions. One important function of N-MYC is the ability of N-MYC to bind its target genes, and our research indicates that preventing the interaction of N-MYC with its co-factor WDR5 can modulate this critical ability of N-MYC. WDR5, with its well-defined “druggable” surfaces that can be used to design small molecule inhibitors, could be an excellent alternative target to restrict N-MYC binding to its target genes.

In this thesis, we demonstrate, using multiple cell lines, that N-MYC and WDR5 co-localize at specific sets of genes across the genome and that WDR5 can recruit N-MYC to chromatin at these genes. Disabling the ability of N-MYC to bind WDR5, via

either utilization of WDR5 degradation or specific WBM mutation, led to reduced ability of N-MYC to bind chromatin at conserved target sites. Importantly, the loci examined are linked to the promoters of genes controlling various cellular processes such as protein synthesis, cell proliferation, and mRNA nuclear export. These genes can collectively induce cancer if not strictly regulated (19), and we predict that blocking N-MYC mediated function at these genes could have a therapeutic impact as what is shown for lymphomas (19). Furthermore, WDR5 recruits N-MYC to many sites known to encode ribosomal protein subunits, which is essential for protein synthesis and subsequent biomass accumulation. Because protein synthesis is a common tumorigenic mechanism for the MYC family (19), these data further support that MYC inhibition through focusing on modulating WDR5 could be an important focal point to anti-cancer therapy research.

The dTAG and Tet-on systems were different in their effect on N-MYC binding, although the ability of N-MYC to bind chromatin was reduced following both approaches. The reduction in N-MYC chromatin binding when N-MYC could not bind to WDR5 was more drastic when the N-MYC-WDR5 interaction was blocked using specific mutations versus broad removal of WDR5 by the dTAG approach. It is possible, even though WDR5 was only degraded for 4 hours in the dTAG experiment (Figure 7), that N-MYC binding was stabilized due to some unknown secondary effect as a consequence of complete WDR5 loss in the cell. It is also possible that in N-MYC amplified cells, the impact of WDR5 on facilitated recruitment of N-MYC is not as robust due to N-MYC

amplification driving high levels of N-MYC. Regardless, reduction in N-MYC binding was observed across both approaches. Future studies will be required to ascertain whether the observed changes in N-MYC chromatin binding impact various aspects of the cell and its functions, such as transcriptional rates at N-MYC-WDR5 target genes or overall cell survival.

Proteins in the human MYC family, including N-MYC, c-MYC, and L-MYC, are all known to interact with WDR5 (18), and MYC amplification is present in a plethora of cancer types (6). Therefore, our experimental approach involving the MYC-WDR5 relationship should continue to be explored in various tumor types and forms of MYC besides exclusively N-MYC and neuroblastoma. Small molecule inhibitors of the Win site of WDR5 have been heavily researched for therapeutic drug discovery in the last several years, and future studies in neuroblastoma may want to understand the utility of these inhibitors for the N-MYC amplified cell lines. However, in this case, a therapeutic window must be discovered to maintain health in non-cancerous cells (27).

In sum, the N-MYC-WDR5 interaction is a promising and hopeful avenue to pursue for discovery of additional novel mechanisms to effectively reduce N-MYC chromatin binding, in hopes of treating high-risk neuroblastoma and a wide variety of malignancies in a clinical setting.

REFERENCES

- (1) St. Jude's Children Research Hospital. *Neuroblastoma*. Available from:
<https://www.stjude.org/disease/neuroblastoma.html> [Accessed 14 Feb 2022].
- (2) Memorial Sloan Kettering Cancer Center. *Symptoms of Neuroblastoma*. Available from: <https://www.mskcc.org/pediatrics/cancer-care/types/neuroblastoma/symptoms-neuroblastoma> [Accessed 14 Feb 2022].
- (3) American Cancer Society. *Treating Neuroblastoma*. Available from:
<https://www.cancer.org/cancer/neuroblastoma/treating.html> [Accessed 14 Feb 2022].
- (4) United Therapeutics Oncology. What Is Neuroblastoma? Available from:
<https://www.neuroblastoma-info.com/what-is-neuroblastoma/> [Cited 2022 Jul 08].
- (5) Pistoia V, Morandi F, Pezzolo A, Raffaghello L, Prigione I. *MYCN: from oncoprotein to tumor-associated antigen*. *Front Oncol* [Internet]. 2012;2:174. Available from: <http://dx.doi.org/10.3389/fonc.2012.00174>
- (6) Tansey W. *Mammalian MYC Proteins and Cancer* [Internet]. *New Journal of Science*. 02Feb2014. Volume 2014, Article ID 757534: Pages 1-27. Available from:
<https://www.hindawi.com/journals/njos/2014/757534/>
- (7) National Center for Biotechnology Information. *MYCN proto-oncogene, bHLH transcription factor [Homo sapiens(human)]*. Available from:
<https://www.ncbi.nlm.nih.gov/gene/4613> [Accessed 28 Sep 2022].

- (8) Beltran H. The N-myc oncogene: Maximizing its targets, regulation, and therapeutic potential. *Mol Cancer Res* [Internet]. 2014;12(6):815–22. Available from: <http://dx.doi.org/10.1158/1541-7786.MCR-13-0536>
- (9) Corvi R, Savelyeva L, Schwab M. *Duplication of N-MYC at its resident site 2p24 may be a mechanism of activation alternative to amplification in human neuroblastoma cells*. *Cancer Res*. 1995;55(16):3471–4.
- (10) Dang CV, Reddy EP, Shokat KM, Soucek L. *Drugging the 'undruggable' cancer targets*. *Nature Reviews Cancer* [Internet]. 2017 Jun 23 [cited 2022 Feb 14];17(8):502-8. Available from: <https://doi.org/10.1038/nrc.2017.36>
- (11) Gori F, Demay MB. BIG-3, a novel WD-40 repeat protein, is expressed in the developing growth plate and accelerates chondrocyte differentiation in vitro. *Endocrinology* [Internet]. 2004;145(3):1050–4. Available from: <http://dx.doi.org/10.1210/en.2003-1314>
- (12) Wysocka J, Swigut T, Milne TA, Dou Y, Zhang X, Burlingame AL, et al. WDR5 associates with histone H3 methylated at K4 and is essential for H3 K4 methylation and vertebrate development. *Cell* [Internet]. 2005;121(6):859–72. Available from: <http://dx.doi.org/10.1016/j.cell.2005.03.036>
- (13) Guarnaccia AD, Tansey WP. Moonlighting with WDR5: A cellular multitasker. *J Clin Med* [Internet]. 2018;7(2). Available from: <http://dx.doi.org/10.3390/jcm7020021>
- (14) Cai WL, Chen JF-Y, Chen H, Wingrove E, Kurley SJ, Chan LH, et al. Human WDR5 promotes breast cancer growth and metastasis via KMT2-independent

translation regulation. *Elife* [Internet]. 2022;11. Available from:

<http://dx.doi.org/10.7554/eLife.78163>

- (15) Kim J-Y, Banerjee T, Vinckevicius A, Luo Q, Parker JB, Baker MR, et al. A role for WDR5 in integrating threonine 11 phosphorylation to lysine 4 methylation on histone H3 during androgen signaling and in prostate cancer. *Mol Cell* [Internet]. 2015;58(3):557. Available from:
<http://dx.doi.org/10.1016/j.molcel.2015.04.030>
- (16) National Center for Biotechnology Information. *WDR5 WD repeat domain 5 [Homo sapiens (human)]*. Available from:
<https://www.ncbi.nlm.nih.gov/gene?Db=gene&Cmd=ShowDetailView&TermToSearch=11091> [Accessed 14 Feb 2022].
- (17) Trievel RC, Shilatifard A. WDR5, a complexed protein. *Nat Struct Mol Biol* [Internet]. 2009;16(7):678–80. Available from:
<http://dx.doi.org/10.1038/nsmb0709-678>
- (18) Thomas LR, Wang Q, Grieb BC, Phan J, Foshage AM, Sun Q, et al. *Interaction with WDR5 promotes target gene recognition and tumorigenesis by MYC*. *Mol Cell* [Internet]. 2015;58(3):440–52. Available from:
<http://dx.doi.org/10.1016/j.molcel.2015.02.028>
- (19) Thomas LR, Adams CM, Wang J, Weissmiller AM, Creighton J, Lorey SL, Liu Q, Fesik SW, Eischen CM, Tansey WP. *Interaction of the oncoprotein transcription factor MYC with its chromatin cofactor WDR5 is essential for tumor maintenance*. *Proceedings of the National Academy of Sciences* [Internet]. 2019

Nov 25 [cited 2022 Feb 14];116(50):25260-8. Available from:

<https://doi.org/10.1073/pnas.1910391116>

- (20) Bryan AF, Wang J, Howard GC, Guarnaccia AD, Woodley CM, Aho ER, et al. *WDR5 is a conserved regulator of protein synthesis gene expression*. *Nucleic Acids Res* [Internet]. 2020;48(6):2924–41. Available from: <http://dx.doi.org/10.1093/nar/gkaa051>
- (21) Walton JD, Kattan DR, Thomas SK, Spengler BA, Guo H-F, Biedler JL, et al. Characteristics of stem cells from human neuroblastoma cell lines and in tumors. *Neoplasia* [Internet]. 2004;6(6):838–45. Available from: <http://dx.doi.org/10.1593/neo.04310>
- (22) Nabet B, Roberts JM, Buckley DL, Paulk J, Dastjerdi S, Yang A, et al. The dTAG system for immediate and target-specific protein degradation. *Nat Chem Biol* [Internet]. 2018;14(5):431–41. Available from: <http://dx.doi.org/10.1038/s41589-018-0021-8>
- (23) Reddy UR, Venkatakrishnan G, Roy AK, Chen J, Hardy M, Mavilio F, Rovera G, Pleasure D, Ross AH. *Characterization of Two Neuroblastoma Cell Lines Expressing Recombinant Nerve Growth Factor Receptors*. *Journal of Neurochemistry* [Internet]. 1991 Jan [cited 2022 Feb 15];56(1):67-74. Available from: <https://doi.org/10.1111/j.1471-4159.1991.tb02563.x>
- (24) Guarnaccia AD, Weissmiller AM, Tansey WP. Gene-specific quantification of nascent transcription following targeted degradation of endogenous proteins

in cultured cells. STAR Protocols [Internet]. 2021;2(4):101000. Available from:
<https://www.sciencedirect.com/science/article/pii/S2666166721007061>

- (25) Weissmiller AM, Wang J, Lorey SL, Howard GC, Martinez E, Liu Q, et al. Inhibition of MYC by the SMARCB1 tumor suppressor. Nat Commun [Internet]. 2019;10(1):2014. Available from: <http://dx.doi.org/10.1038/s41467-019-10022-5>
- (26) Sangaré L, Morisset R, Omri A, Ravaoarino M. Incorporation rates, stabilities, cytotoxicities and release of liposomal tetracycline and doxycycline in human serum. J Antimicrob Chemother [Internet]. 1998;42(6):831–4. Available from: <http://dx.doi.org/10.1093/jac/42.6.831>
- (27) Wang F, Jeon KO, Salovich JM, Macdonald JD, Alvarado J, Gogliotti RD, et al. Discovery of potent 2-aryl-6,7-dihydro-5 H-pyrrolo[1,2- a]imidazoles as WDR5-WIN-site inhibitors using fragment-based methods and structure-based design. J Med Chem [Internet]. 2018;61(13):5623–42. Available from: <http://dx.doi.org/10.1021/acs.jmedchem.8b00375>